

Functional localization of auditory cortical fields of human: Click-train stimulation

John F. Brugge^{a,b,c,*}, Igor O. Volkov^a, Hiroyuki Oya^a, Hiroto Kawasaki^a,
Richard A. Reale^{a,c}, Albert Fenoy^a, Mitchell Steinschneider^{d,e}, Matthew A. Howard III^a

^a Department of Neurosurgery, University of Iowa College of Medicine, Iowa City, IA 52242, United States

^b Department of Physiology, University of Wisconsin, Madison, WI 53705, United States

^c Department of Psychology, University of Wisconsin, Madison, WI 53705, United States

^d Department of Neurology, Albert Einstein College of Medicine, New York, NY 10461, United States

^e Department of Neuroscience, Albert Einstein College of Medicine, New York, NY 10461, United States

Received 29 August 2007; received in revised form 28 November 2007; accepted 30 November 2007

Available online 8 December 2007

Abstract

Averaged auditory evoked potentials (AEPs) to bilaterally presented 100 Hz click trains were recorded from multiple sites simultaneously within Heschl's gyrus (HG) and on the posterolateral surface of the superior temporal gyrus (STG) in epilepsy-surgery patients. Three auditory fields were identified based on AEP waveforms and their distribution. Primary (core) auditory cortex was localized to posteromedial HG. Here the AEP was characterized by a robust polyphasic low-frequency field potential having a short onset latency and on which was superimposed a smaller frequency-following response to the click train. Core AEPs exhibited the lowest response threshold and highest response amplitude at one HG site with threshold rising and amplitude declining systematically on either side of it. The AEPs recorded anterolateral to the core, if present, were typically of low amplitude, with little or no evidence of short-latency waves or the frequency-following response that characterized core AEPs. We suggest that this area is part of a lateral auditory belt system. Robust AEPs, with waveforms demonstrably different from those of the core or lateral belt, were localized to the posterolateral surface of the STG and conform to previously described field PLST.

© 2008 Elsevier B.V. All rights reserved.

Keywords: Human auditory cortex; Heschl's gyrus; Auditory evoked potential

1. Introduction

Human auditory cortex is composed of multiple fields distributed both on the exposed surface of the superior temporal gyrus (STG) and in areas buried within the Sylvian fissure beneath the overlying parietal cortex on the supratemporal plane. The numbers, locations and boundaries of the fields are not well known nor are homologies with cortical auditory fields of non-human primates

well delineated. Cytoarchitectonic studies have consistently identified a patch of koniocortex confined to the posteromedial portion of the transverse temporal gyrus of Heschl (HG) that is also heavily myelinated and exhibits a distinct chemoarchitecture (reviewed by Hackett, 2003). Although traditionally considered the site of the primary auditory field (AI), this area is not homogeneous in its cellular architecture (Galaburda and Sanides, 1980; Morosan et al., 2001; Fullerton and Pandya, 2007) suggesting that it may represent more than one primary or 'primary-like' field and, thus, may better be considered a primary cortical complex or, as in monkey, an auditory core (Hackett et al., 2001). Anatomical studies have also consistently shown a belt of cortical fields on the superior temporal

* Corresponding author. Address: Department of Psychology, Brogden Hall, 1210 W. Johnson Street, University of Wisconsin, Madison, WI 53705, United States. Tel.: +1 608 263 5928; fax: +1 608 263 5929.

E-mail address: Brugge@physiology.wisc.edu (J.F. Brugge).

plane adjacent to, and distinct from, the core koniocortex. Although there is not full agreement on the number and locations of belt fields, as many as seven have been identified on histochemical grounds (Rivier and Clarke, 1997; Wallace et al., 2002). One or two auditory fields have been identified lateral to belt fields, on the posterolateral exposed surface of the STG (Wallace et al., 2002; Sweet et al., 2005).

Auditory evoked potentials (AEPs) obtained in response to a wide range of both simple and complex sound have been recorded directly from the superior temporal plane of neurosurgical patients both acutely in the operating room (Sem-Jacobsen et al., 1956; Chatrian et al., 1960; Celesia and Puletti, 1969; Celesia and Puletti, 1971; Puletti and Celesia, 1970; Celesia, 1976) or chronically through implanted multi-channel depth electrodes (Lee et al., 1984; Liegeois-Chauvel et al., 1991, 1994; Howard et al., 1996b, 2000; Steinschneider et al., 1999; Steinschneider et al., 2005; Fishman et al., 2001; Yvert et al., 2002, 2005; Trebuchon-Da Fonseca et al., 2005; Bidet-Caulet et al., 2007). In cases where there was adequate anatomical localization of recording sites, these AEPs were localized to a relatively restricted area of posteromedial HG, which was taken to be the primary auditory field. Robustly-responsive, frequency-tuned and tonotopically-organized neurons and neuronal clusters were recorded in cortex of the posteromedial HG by Howard et al. (1996b), which provided direct evidence for this area being considered field AI. In comparison to posteromedial HG, waveforms recorded more anterolaterally are dominated by AEPs of relatively longer latency and lower amplitude (Celesia, 1976; Liegeois-Chauvel et al., 1991, 1994) signaling perhaps a second auditory field on HG adjacent to the auditory core. Additionally, AEPs recorded directly from the posterolateral STG exhibit waveforms and response sensitivity demonstrably different from that recorded on HG, and on this basis we earlier referred to the area as the posterolateral superior temporal auditory field (area PLST, Howard et al., 2000; Brugge et al., 2003, 2005).

Although many questions still remain unanswered regarding homologies with auditory cortical fields of non-human primates (Hackett et al., 2001; Hackett, 2003; Sweet et al., 2005), studies of auditory cortex in monkey continue to guide research in human (see Scott, 2005). Based on cellular architecture, patterns of connections and tone-frequency maps, a dozen or more auditory or auditory-related fields have been identified in monkey and broadly grouped into four processing levels (Kaas and Hackett, 2000). A core of as many as three koniocortical fields, including AI, on the supratemporal plane is flanked by perhaps seven auditory belt fields. Belt fields project topographically upon two or more parabelt fields which, in turn, make connections with more distant cortex of the temporal, parietal and frontal lobes. A hierarchical serial/parallel processing model derived from anatomical and physiological studies of these fields posits that information about spectro-temporal features of a natural sound are pre-

served in core cortex and from there disseminated to belt and parabelt fields where through convergent and divergent interactions they are transformed and integrated into more complex cerebral representations (Rauschecker, 1998; Kaas and Hackett, 2000). Although there is general agreement that the auditory core koniocortex in human is homologous to that of the non-human primate, far less certain are homologies regarding belt and parabelt fields (Hackett et al., 2001; Hackett, 2003; Sweet et al., 2005; Fullerton and Pandya, 2007). Nonetheless, evidence from fMRI studies suggests that a functional hierarchy may also exist for human auditory cortex (Wessinger et al., 2001), which may be incorporated into dual-stream models of cortical processing of complex sound, including speech (Rauschecker and Tian, 2000; Griffiths et al., 2004; Hickok and Poeppel, 2004, 2007). Thus, while the non-human primate model of auditory cortical processing continues to be useful in guiding human studies, it is essential to carry out studies directly in humans using a variety of complementary experimental approaches if we are to understand fully the functional organization of human auditory cortex and especially the mechanisms underlying the perception of speech and other complex sound.

Our aim is to localize and characterize physiologically the auditory cortical fields of the STG in the human. Our approach in doing so is to record directly from auditory cortex of epilepsy-surgery patients while they listen, and in some cases respond behaviorally, to a wide range of controlled sounds. In this paper we describe the results of a series of experiments in which the AEPs to a brief click train (5 clicks at 100 Hz) were recorded simultaneously through multi-contact electrodes chronically implanted within HG and on the exposed surface of the posterolateral STG. Using this stimulus we were able to distinguish one field from another based not only on the waveform of the AEP evoked by the abrupt onset of the click train but also by the synchronized, frequency-following, response (FFR) to individual clicks in the train. By mapping the distribution AEPs and the FFR, and relating these waveforms to anatomically confirmed recording locations, we have identified at least three auditory cortical fields – two on HG and a third on the posterolateral surface of the STG.

2. Materials and methods

Studies have been carried out on 25 patients undergoing evaluation to identify a seizure focus prior to surgery aimed at alleviating their medically intractable epilepsy. Research protocols were approved by the University of Iowa Human Subjects Review Board. Prior informed consent was obtained from each patient enrolled in the study. As part of the treatment plan depth electrodes were inserted into HG on the supratemporal plane while grid electrodes were implanted over perisylvian cortex of the left hemisphere in seven and the right hemisphere of 18 patients. The depth electrodes were modified slightly for experimental purposes (Howard et al., 1996a). WADA-test results showed

left-hemisphere language dominance for all patients. All patients had standard audiometric testing prior to implantation surgery, and none showed hearing impairment that would impact the findings reported here. Clinical EEG evaluation indicated that neither HG nor adjacent auditory cortical tissue was the site of the epileptogenic foci.

The modified hybrid depth electrodes (HDEs) were targeted stereotactically for the left or right HG. HDEs carried four or six macro-contacts (impedance approx. 5 k Ω measured in situ) consisting of 1.6 mm circumferential platinum spaced 10 mm apart. These contacts recorded both clinical EEG data and sound-evoked local field potentials. The recording reference for these contacts was a platinum disc in contact with the undersurface of the ipsilateral anterior temporal lobe or with the galea near the vertex of the skull. Sixteen micro-contacts (impedance approx. 0.08–0.2 M Ω measured in situ), consisting of 40- μ m wires with exposed ends cut flush with the electrode shaft, were distributed at 1–2 mm intervals between the macro-contacts. The reference for the micro-contacts was the same as that for the macro-contacts or was one of the two most distal micro-contacts near the lateral surface of the STG. In all cases, contributions to the AEPs from activity at the reference sites were negligible. The HDE was oriented roughly parallel to the long axis of HG in all cases, thereby allowing us to record activity from as many as 22 sites distributed along its length. Electrodes remained in place for 7–14 days.

Each patient underwent whole-brain MR imaging prior to implant surgery, and nine of them underwent CT scanning as well. To locate recording contacts on the HDEs, high-resolution T1-weighted structural MRIs (in-plane resolution: 0.87 \times 0.87 \times 1.5 mm or 0.78 \times 0.78 \times 1.0 mm) were obtained both before and after electrode implantation. Post-implantation MRIs were obtained usually one day before electrode removal. Pre- and post-implantation MRIs were co-registered using a 3-D rigid-fusion algorithm implemented in Analyze software (Biomedical Imaging Resource, Mayo Clinic). Coordinates for each electrode contact obtained from post-implantation MRI volumes were then transferred to pre-implantation MRI volumes. The location of every contact relative to visible surrounding brain structures was compared in both pre- and post-implantation MRI volumes. Implantation of electrodes displaces the cerebral hemisphere medially with superficial brain tissue being distorted more than deeper structures. This non-linear compression causes the depiction of electrode trajectory and the spacing of contacts, when transferred to the pre-operative images, appear irregular, as in Figs. 1, 3, 5 and 6). Serial MR cross-sectional images containing each of the recording contacts were obtained at roughly right angles to the trajectory of the HDEs, and the coordinates of the electrode shaft were determined by means of a program implemented in MATLAB (Mathworks, MA). Surface renderings of the supratemporal plane with loci of HDE contacts projected on them as well as line drawings of each cross section outlining the grey matter and the position of the electrode at that location were created.

It has been known probably from the time of Heschl's original 1878 description of the supratemporal plane that more than one transverse gyrus may be present and separated by intermediate sulci (see Bailey and Bonin, 1951 for the early historical record). MRI renderings of the supratemporal plane in 23 of 25 of our subjects were adequate to determine that a single transverse gyrus was present in 5 of 7 left hemispheres and 12 of 16 right hemispheres. When more than one transverse gyrus was present, the HDE was found to have traversed the most anterior one, which is known from cytoarchitectonic studies to be the location of auditory koniocortex.

HDEs are constructed in such a way that all of the micro-contacts from which recordings are obtained are located on one side of the electrode shaft. Thus, while we are confident of the anatomical location of our recording sites within the HG, the MR images used in the electrode-tract reconstruction are not adequate to identify the cortical laminae in which these recording contacts lay. The MRI electrode reconstruction showed that in 14 of 25 patients all of the HDEs were in contact with the HG grey matter. In several other patients a portion of the HDE was in the grey matter, with the remainder lying within the underlying white matter. In this paper we present data only from those electrode contacts that were confirmed by our anatomical analyses to be within the HG grey matter. Localization of the subdural surface grid contacts was aided by digital photographs taken in the operating room at the time of implantation and by surface renderings of the grid superimposed on the pre-implantation MRI. At the time of electrode removal the locations of the grids was confirmed and again photographically documented.

The acoustic stimulus was a train of five rectangular pulses (0.2 ms wide, 10 ms interval) presented bilaterally every 2 s by means of insert earphones (ER4B, Etymotic Research, Elk Grove Village, ILL) integrated into custom fitted ear molds of the kind commonly worn by hearing aid users. In three experiments the effects of stimulus level on the AEPs was studied. In all other cases, the stimulus was held at a comfortable level, about 30–50 dB above hearing threshold. AEPs were recorded from macro- and micro-contacts of the HDEs and from grid contacts to repeated stimulation ($n = 50$ or 100). Depending on the data acquisition system used (DataWave, Hewlett Packard, Tucker Davis Technologies) and whenever possible, these recordings were made simultaneously in an attempt to reduce the inevitable variability that would occur over successive recording sessions. Signals were amplified, filtered (1–1000 Hz) and digitized on-line at sampling rates of 2000–25,000 Hz. Digitized data were stored for later off-line analysis. Recordings were carried out in the epilepsy monitoring unit of University of Iowa Hospital and Clinics or in specially designed and constructed electrophysiological recording suites in the University of Iowa General Clinical Research Center. In all cases, during experimental recording sessions the subjects were awake and sitting comfortably in their hospital bed or in a nearby chair.

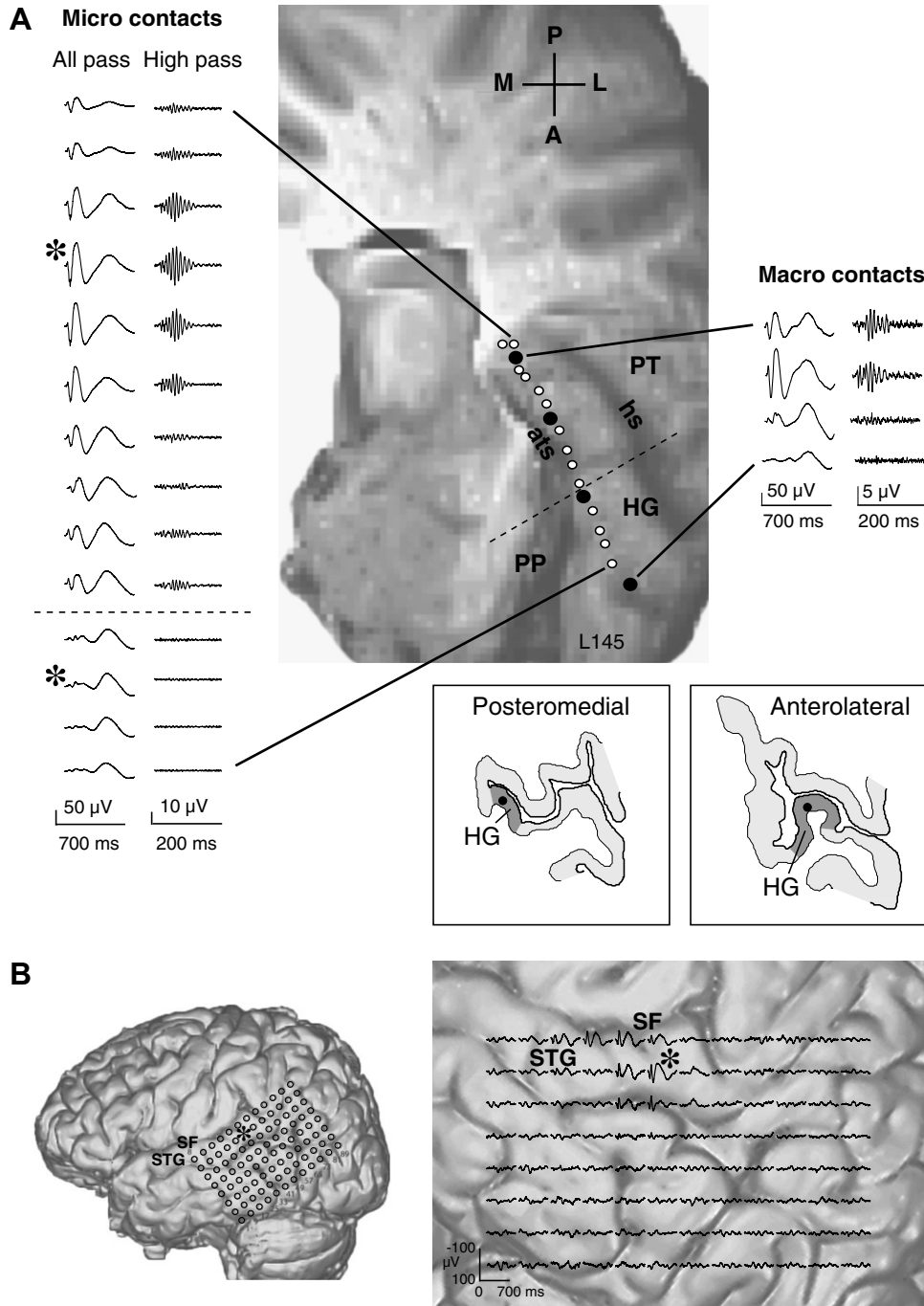


Fig. 1. (A) AEPs recorded from 14 micro-contact and four macro-contact sites along the length of HG of the left hemisphere of one subject. In this and subsequent figures negative voltage is plotted upward. AEPs in left column were filtered from 1.6 to 1000 Hz, those in right column from 70 to 1000 Hz. Asterisk marks two sites of maximal amplitude of response, in posteromedial and anterolateral HG. Dashed line denotes where a functional transition takes place in the sequence of AEPs. Drawings of MRI cross sections show the position of the recording electrode (closed black circle) within the grey matter (light grey shading) at the two representative recording locations marked with the asterisk. Dark grey shading denotes the estimated medio-lateral extent of HG. The electrode trajectory and location of each recording site are shown on the surface rendering of the superior temporal plane. Open circles: micro contacts; closed circles: macro contacts; HG: Heschl's gyrus; ats: anterior transverse sulcus; hs: Heschl's sulcus; PT: planum temporale, PP: planum polare. (B) All-pass AEPs recorded from the 96-contact grid on the peri-sylvian cortex. The locations of the recording contacts are shown on the MRI rendering of the lateral surface of the cerebral hemisphere. Expanded view shows the AEPs recorded at each site. SF: Sylvian fissure; STG: superior temporal gyrus.

3. Results

Two auditory fields on HG and one on the posterolateral surface of the STG were distinguished based on the charac-

teristics of the waveforms evoked by the 100 click-train stimulus. Fig. 1 illustrates activity recorded from these fields in one patient whose AEPs were obtained simultaneously from 14 micro-contacts and four macro-contacts on a

HDE that traversed, within gray matter, the long axis of HG, and from 96 contacts of a grid overlaying the posterolateral STG. Recordings were made on the left hemisphere. Waveforms recorded at macro-contact sites were not demonstrably different from those recorded at their nearest-neighbor micro-contact site. All-pass (1.6–1000 Hz) filtered AEPs are shown with their respective high-pass (70–1000 Hz) filtered versions. The electrode remained in grey matter near the crest of HG over its entire trajectory as seen from the surface rendering of the supratemporal plane and from tracings of the MRI cross sections containing a poster-

omedial and an anterolateral micro-contact recording site from which AEPs exhibiting greatest amplitude were obtained. Below is shown the distribution of 96 all-pass filtered AEPs overlaid on the surface MRI rendering. Details of all-pass and high-pass filtered AEP waveforms are shown in Fig. 2, at different temporal resolutions (note changing time scale).

Robust, polyphasic AEPs were recorded within about the posteromedial two-thirds of HG (Fig. 1A). The all-pass AEP exhibiting the greatest amplitude appeared at one posteromedial recording site (asterisk). The waveform

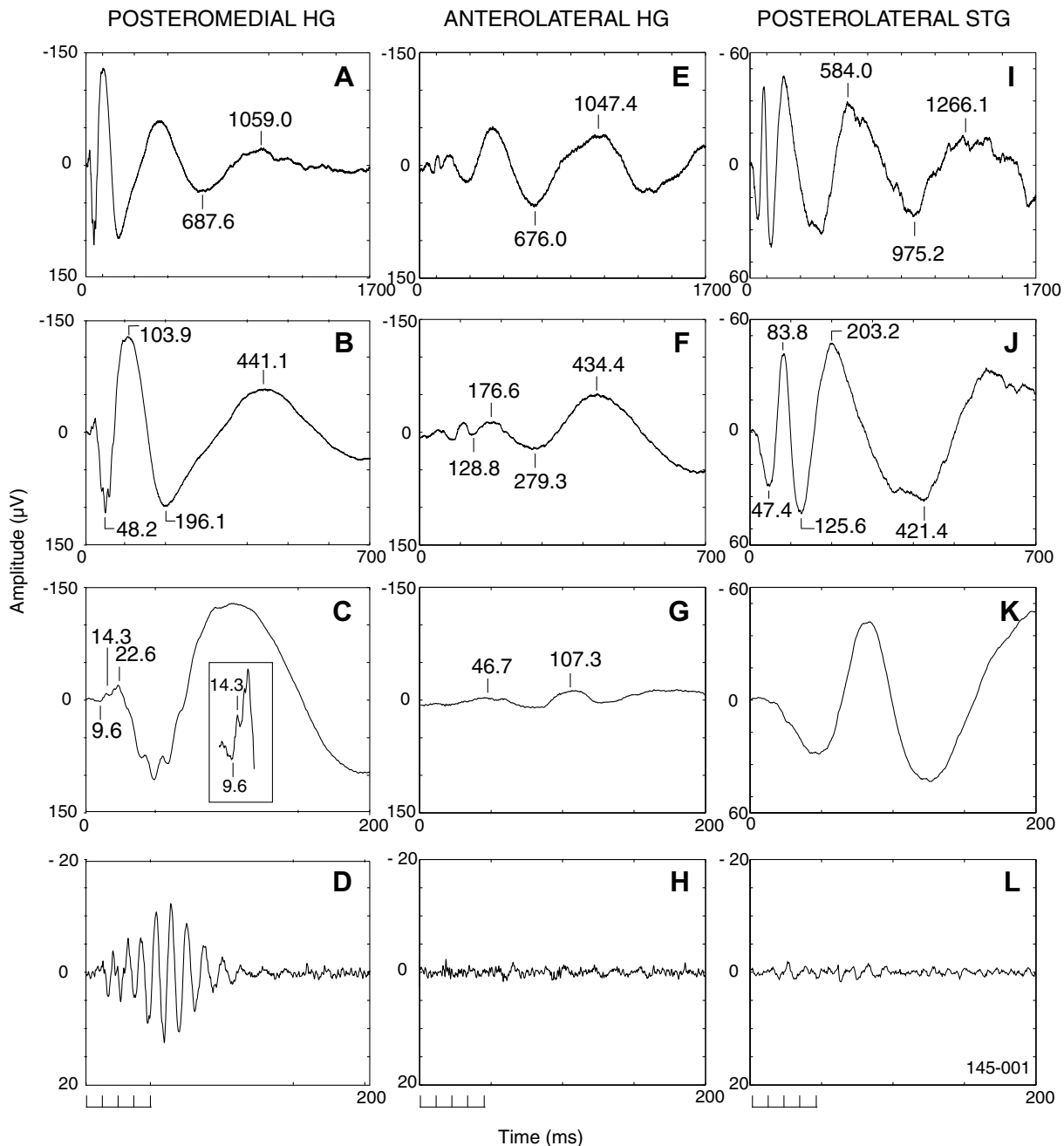


Fig. 2. AEP waveforms obtained at the sites of maximal amplitude on posteromedial (A–D) and anterolateral (E–G) HG and from posterolateral STG (I–L) plotted at different time scales. Filters: 1.6–1000 Hz for all but D, H, L, for which a high-pass filter (70–1000 Hz) was employed. Latency (ms) of major deflections shown on figures.

obtained at this site was characterized by its short onset latency (9.6 ms), large positive–negative voltage deflections within about the first 200 ms after stimulus onset, and a later broad positive deflection around 400 ms (Fig. 2B and C). In this experiment we obtained the AEP for the full 2 s after stimulus onset, which revealed peaks in the waveform with latencies exceeding 1 s (Fig. 2A). Other than to note their occurrence we have not sufficient data to comment on them further. On either side of this site of maximal responsiveness, the amplitudes of early (below about 200 ms) deflections fell off systematically, although the shape of the AEP remained relatively constant. The amplitude of the relatively late, broad, negative deflection also declined posteromedially but remained in evidence at anterolateral sites.

Superimposed on the all-pass waveform are smaller deflections that are related to the periodicity of the click train (Fig. 2A–C). These deflections, which are more clearly seen when the AEP is high-pass filtered, contain a frequency-following response (FFR) in addition to other higher-frequency components evoked by the click train (Fig. 2D). For the purposes of this study we refer to the entire high-pass filtered response complex as the FFR, and show that it may serve as a physiological marker identifying an auditory field on posteromedial HG. The greatest amplitude of the FFR occurred at or near the site of maximal amplitude of the all-pass AEP and, like the all-pass AEP amplitude, that of the FFR fell off on either side of this site.

The early deflections of the all-pass filtered AEP decreased abruptly in amplitude further anterolaterally leaving a later negative deflection to dominate the response, including one with a peak of around 1 s. Moreover, there was no longer evidence of a FFR (Fig. 2H). We take these transitions in the AEP along the linear array of contacts on the HDE to mean that we had recorded simultaneously from two auditory fields, one on posteromedial HG and the other on anterolateral HG. The location and responsiveness of the former is consistent with it being a part of the auditory core, whereas the latter may be interpreted as being part of the auditory belt. The dashed line in Fig. 1A denotes what we interpret as a functional boundary between the two fields.

Simultaneous with the HG recordings, a cluster of polyphasic AEPs was recorded on the dorsal aspect of the posterolateral exposed surface of the STG. A site of maximal AEP amplitude (asterisk) and a gradient of response magnitude was seen here (Fig. 1B). The waveforms recorded here differed demonstrably from those recorded on HG (Fig. 2I–L) and, thus, characterized a possible third auditory field – the posterolateral superior temporal auditory field (PLST) – which we described earlier (Howard et al., 2000; Brugge et al., 2003, 2005). Although similar data were obtained from posterolateral STG in all patients studied, we will focus attention on results obtained from HG recordings.

The general findings described in Figs. 1 and 2 were obtained in all subjects studied, although there was inter-

subject variability in the shapes and spatial distributions of the AEPs. This can be seen by comparing the map shown in Fig. 1A with that in Fig. 3, which was obtained from the right hemisphere of another subject. In this case the electrode traversed, within grey matter, the medial edge of HG and failed to reach the most posteromedial portion of the gyrus. The all-pass AEP obtained at the six most posteromedial recording sites exhibited an early polyphasic waveform followed by an even larger broad negative deflection, around 400 ms. The high-pass filtered waveform exhibited an FFR to the click train at these six sites. The amplitude of the early all-pass AEP and the FFR exhibited a decrease in amplitude with distance from the site of maximal response amplitude (asterisk). A relatively abrupt change in amplitude signaled a transition (dashed line) to responses characterized by a dominant late negativity and decrement of the FFR.

The range of inter-subject variability in the AEPs recorded in our experiments is illustrated further in Fig. 4, which depicts the AEPs obtained at the site of maximal amplitude of response for 12 subjects in which the electrode was shown to be within grey matter of HG. While the latency of the prominent peaks and valleys in the waveforms were consistent within a given subject, they varied considerably from one subject to the next. The left column

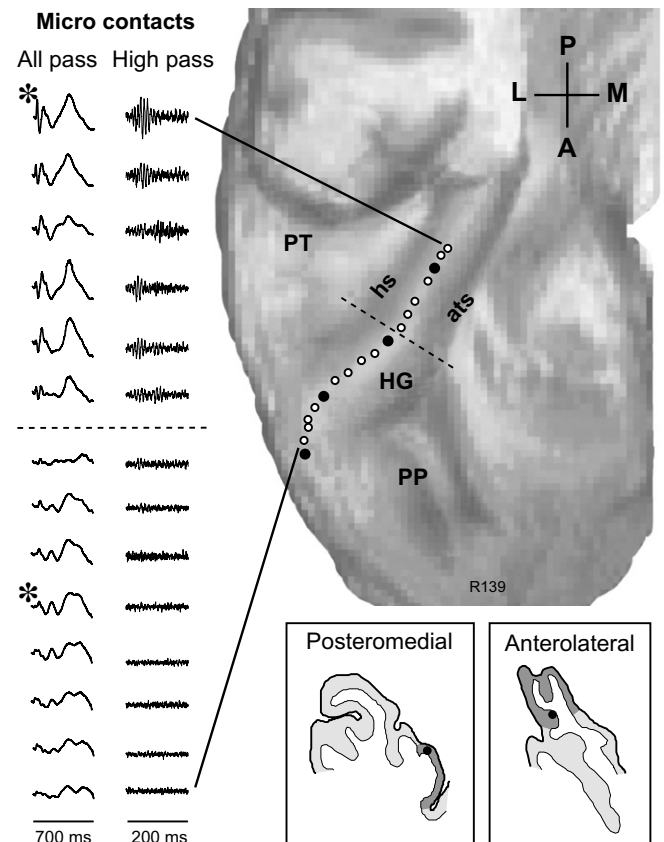


Fig. 3. AEPs recorded from 14 micro-contact and four macro-contact sites along the length of HG of the right hemisphere. See legend of Fig. 1 for details.

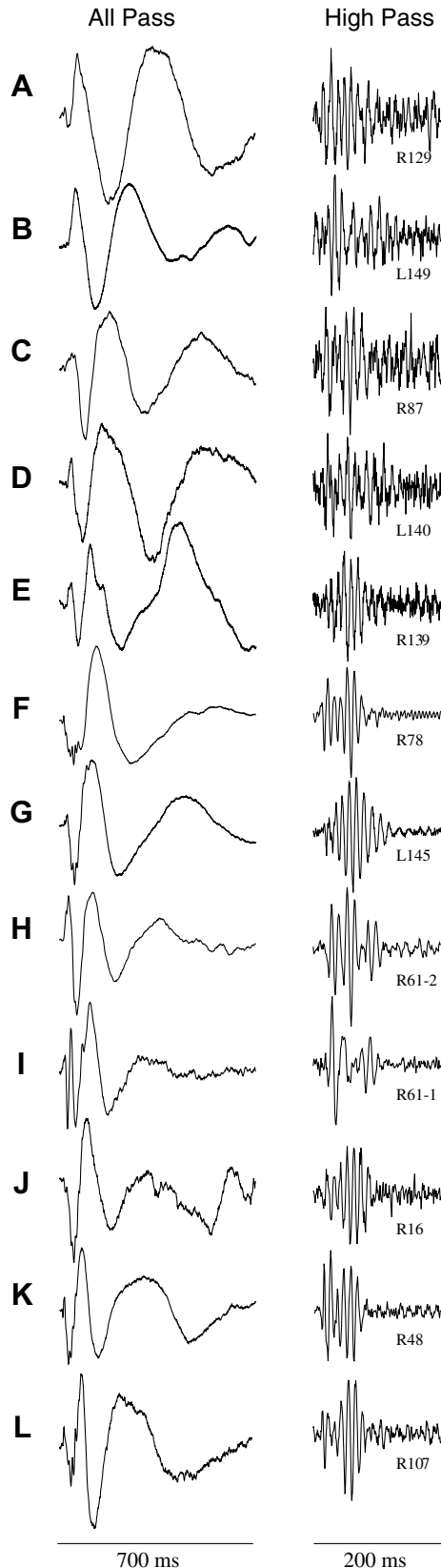


Fig. 4. AEPs obtained at the site of maximal amplitude of response in posteromedial HG of 12 subjects. Left-hand column AEP filter 1.6–1000 Hz, right-hand column 70–1000 Hz. Amplitudes adjusted for comparison of waveforms.

illustrates the all-pass AEPs ordered, by eye, by the latency of the earliest deflections regardless of polarity. It is quite likely that some of the polarity and latency differences shown here are due to the electrode being in different laminae of grey matter or, possibly, in different core fields. Hence, we did not attempt to determine corresponding peaks across subjects, as the inter-subject variability we encountered in the waveforms made it difficult, if not impossible, to do so accurately. The possible exception to this was the earliest deflection, which may be interpreted as being the first sign of the incoming thalamic volley of activity (Steinschneider et al., 1992). It was typically of very low amplitude, but we were able to reliably measure its onset in seven of 13 cases. The onset latency was shortest at the focus of maximal response amplitude and lengthened by several msec over the dynamic range of intensity (see Fig. 5). When measurable (7/13 subjects) at the site of maximal amplitude and at a level where the latency reached a near asymptotic level, the onset latency ranged from 8.0 to 14.0 ms (mean: 10.9 ms). A more prominent early deflection was recorded at 11.5–35.6 ms (mean: 19.1 ms, $n = 12$). The inset of Fig. 2C illustrates for one subject details of these relatively small and very early deflections.

The right-hand column of Fig. 4 illustrates the inter-subject variability in the high-pass filtered versions of these adjacent AEPs. The FFR was identified in all cases, although it was more prominent in some than in others. Although both the all-pass AEP and the FFR shown here were obtained from posteromedial HG, in different subjects they may have been recorded from different laminae, from different subdivisions within the auditory core, or both. The variability may also reflect effects of different acoustic environments and/or seizures which our subjects previously experienced.

Linear mapping results shown so far were obtained at one stimulus level, which was some 30–50 dB above click threshold. To insure that fundamental response patterns were not determined by stimulus intensity, the signal level of the click train was systematically varied in three subjects. Fig. 5 illustrates in a different subject the all-pass AEP and the FFR obtained at the site of maximal amplitude when stimulus level was varied systematically over a range of 90 dB. In this case, recordings were obtained from grey matter near the crest of HG of the right hemisphere. Here we see that both the all-pass AEP and the FFR arose together at a threshold of between 80 and 90 dB attenuation, which is very near the subjects' hearing threshold for the click train. Amplitudes of both grew rapidly over a range of 30–40 dB, while the latency of the earliest positive deflection in the all-pass AEP decreased to a plateau around 60 dB above threshold. Latency of the FFR was difficult to determine, as the response appeared to interact with early waves of the all-pass AEP. Despite intensity related changes in amplitude and onset latency, the basic waveform remained relatively constant.

Intensity-dependency of AEPs recorded from posteromedial HG of two other subjects is shown in Fig. 6. The

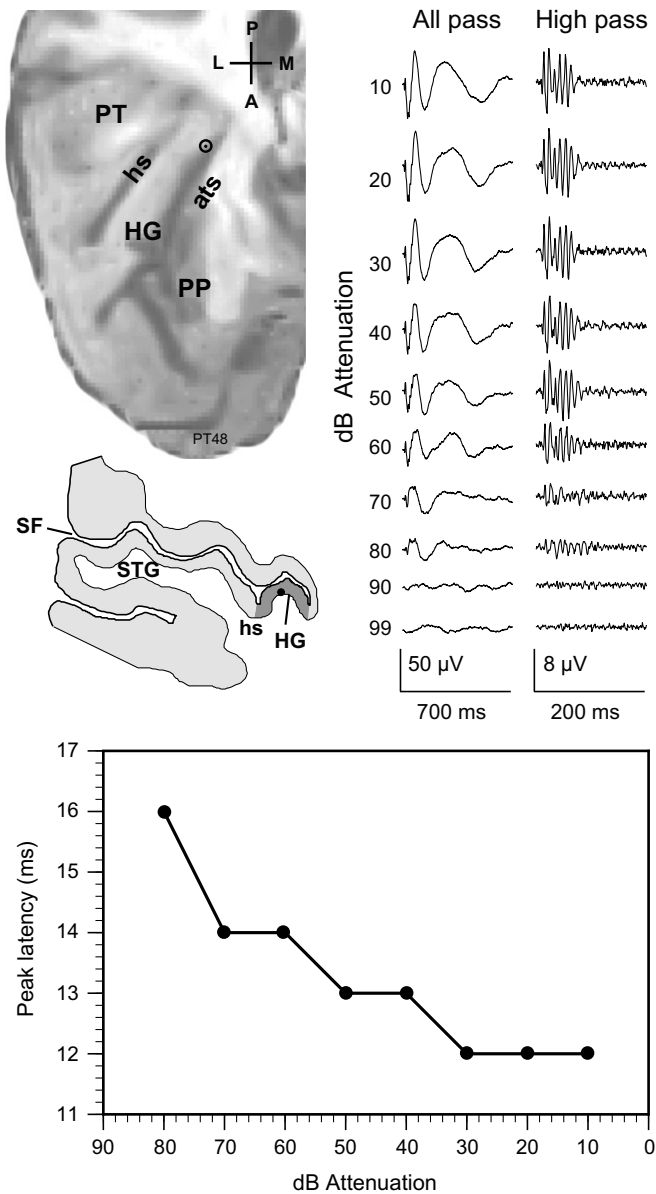


Fig. 5. Effects of changing stimulus level on AEP obtained at the site of maximal amplitude of response on posteromedial HG denoted by a circle on the surface rendering of the supratemporal plane. Drawing of MRI cross section shows electrode within the grey matter near the crown of the gyrus. See legend of Fig. 1 for details.

FRR was embedded in the all-pass AEP, but for clarity of presentation only the all-pass filtered waveform of the AEP is shown. Fig. 6A shows data from the left hemisphere where the electrode traversed the grey matter along the lateral edge of HG almost to its posteromedial border. The shaded area is meant to include those recording sites where AEPs obtained there were clearly above threshold.

At the three highest stimulus levels used (35, 45, 55 dB attenuation) AEPs exhibited very similar waveforms at all recording sites. The greatest amplitude at the three most posteromedial recordings locations, with amplitude falling off systematically with distance from those sites. At 65 dB attenuation there was a decrement in the amplitude of

the AEP at each recording location, and the distance over which it was observed became restricted to the most posteromedial sites around the site of maximal amplitude. Over this range of 30 dB the AEP retained its waveform. At 75 dB attenuation there was little evidence of evoked activity.

Results shown in Fig. 6B, from the right hemisphere of a different subject, exhibit similar properties. In this case the electrode followed the most medial border of all but the most posteromedial aspect of HG. At 45 dB attenuation the five posteromedial contacts recorded robust AEPs while the five most anterolateral sites exhibited but a small late positivity. As the stimulus level was systematically decreased over 40 dB this border appeared to shift in a posteromedial direction, toward the site of maximal response amplitude.

4. Discussion

We have identified what we believe to be three auditory fields on the human STG based on the amplitude and time structure of AEP waveforms recorded in response to 100 Hz click trains. We interpret the activity recorded in posteromedial HG as arising from a primary (core) auditory field. AEPs recorded here are characterized by their relatively large amplitude, short onset latency and a FFR. The amplitude of the AEP, including the FFR, is greatest at one recording location and diminishes with distance from this site. Anterolateral to this core field, but still on HG, is a field we interpret as being part of an auditory belt. The transition from the AEP of the core field to a waveform characterized by low amplitude and predominantly long-latency deflections signals a boundary between this belt field and the auditory core. Lateral to this belt field, on the exposed surface of the posterolateral STG, is a third field, which we earlier tentatively suggested may be part of an auditory parabelt system in humans (Howard et al., 2000; Brugge et al., 2003, 2005) and referred to it as the posterolateral superior temporal auditory field (PLST). As described earlier, field PLST exhibits robust AEPs to a wide range of acoustic stimuli and has response properties that distinguish it from auditory fields on HG. These three fields were identified in all subjects and on both the left and right cerebral hemispheres.

Sem-Jacobsen et al. (1956) and Chatrian et al. (1960) were the earliest investigators to record auditory evoked activity directly from cortex deep within the lateral fissure in humans. Unfortunately, in their studies anatomical reconstructions of the recording electrodes were not carried out to determine accurately the recording locations; thus, directly relating our results to theirs is not possible. Our data are relatively consistent, however, with later intra-operative results of Ceesia (1976) and chronic recordings of Liegeois-Chauvel et al. (1991, 1994) and Godey et al. (2001) when one makes allowance for inter-subject variability and the differences between the studies in electrode

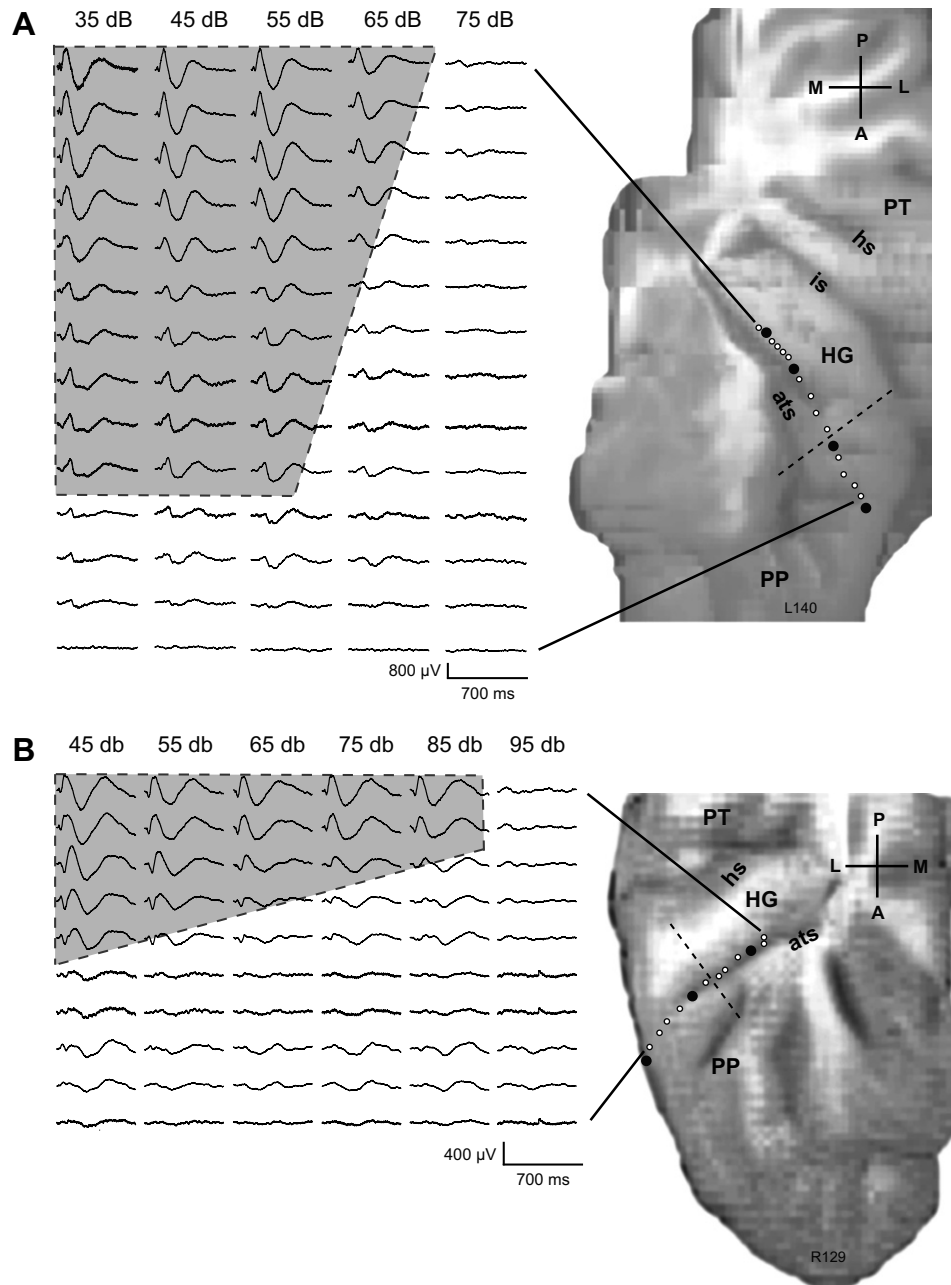


Fig. 6. Effects of changing stimulus level on the AEP map of the left and right HG of two subjects. High-pass filtered AEP omitted for clarity of presentation. See legends of Figs. 1 and 5 for details.

placement, recording methods and methods used to anatomically localize recording sites.

Celesia and colleagues, who recorded click-evoked AEPs from the superior temporal plane during surgery using a multi-contact depth electrode, estimated the location of recording contacts by relating them to their distance from the anterior tip of the temporal lobe and from the exposed surface of the STG. Considering the lack of imaging technology with suitable resolution available at that time, a more accurate localization of recording sites was probably not possible. The summary response map of HG from the Celesia and Pulletti (1976) work was derived

from the data pooled across subjects, an approach that relies upon gross surface landmarks for localizing the recording sites but that does not take into account considerable inter-subject variability in gross and cellular morphology of the supratemporal plane (Bailey and Bonin, 1951; Rademacher et al., 1993, 2001; Leonard et al., 1998). As a result, localization was necessarily blurred and size of the area they illustrated as the primary auditory field is likely larger than a primary field in any given individual. Liegeois-Chauvel and colleagues (1991, 1994), in their chronic recordings, advanced considerably our understanding of auditory localization in HG by introducing

cerebral angiography to obtain three-dimensional coordinates of each HG electrode lead in relationship to the temporal branch of the middle cerebral artery, the insula and the Sylvian fissure. Godey et al. (2001) also carried out anatomical reconstruction of recording sites by visualizing the electrode tracks with stereotaxic MRI after the electrodes had been removed. In all of these studies, the depth electrodes had entered the exposed lateral surface of the STG normal to the gyral surface and, therefore, traversed HG somewhat obliquely. Thus, polarity reversals in the AEP necessarily occurred, which were interpreted as being due to different electrode contacts lying within different cortical laminae with respect to the AEP cortical source dipole (see Arezzo et al., 1975; Steinschneider et al., 1992). Moreover, as data were acquired over multiple recording channels, the activity profile of HG had to be constructed from responses recorded on different electrodes in different subjects.

We have taken a different approach to electrode implantation and subsequent anatomical reconstruction in an attempt to identify auditory fields on the STG and to circumvent problems associated with pooling data across subjects and recording across cortical laminae. In our experiments, multi-channel HDEs were inserted roughly parallel to the long axis of HG, with the intent of maintaining electrode position within the cortical grey matter. This had the advantage that, when successful, the linear array of closely spaced recording contacts was positioned to cross possible field boundaries on HG while maintaining relatively constant positions with respect to the AEP source dipole in the cortical grey matter. We then carried out 3D reconstruction of the electrode tract(s) in each subject, identifying the location of each recording contact. Indeed, in those subjects for which we have anatomical localization of electrode placement within the HG grey matter there was but a single transition in the AEP waveform and no abrupt changes in polarity of the AEP along the electrode trajectory. This suggested to us that in these cases the electrode crossed a field boundary and that the recording contacts remained in relatively constant relationship to the cortical dipoles. Moreover, the multi-contact grid implanted on the posterolateral surface of the STG allowed us to record from PLST simultaneously with HG in order to probe directly for additional fields beyond the superior temporal plane. Thus, by having simultaneous recordings from all contacts on HG and posterolateral STG we also overcame the problems of comparing results from different cortical areas that are necessarily associated with changes taking place in the state of the subject and the subject's auditory cortex between experimental sessions.

The most robust AEPs recorded on HG were located on the posteromedial portion of HG. The all-pass AEPs were characterized by a polyphasic waveform with deflections that appeared at variable peak latency for more than 500 ms after stimulus onset. Typically the AEP was largest and threshold lowest at one recording site with amplitude falling off and threshold rising on either side of this site. Within the first 50 ms or so after stimulus onset the wave-

form of the AEP exhibited several deflections. The earliest deflection had an average onset latency of 10.9 ms, which we take to represent the time of arrival of the first afferent volley from the auditory thalamus evoked by our transient stimulus (Steinschneider et al., 1992). Thus, the shape and the timing of the AEP waveforms, along with their spatial distribution in HG, are consistent with the results of Celesia and Puletti (1976) and with Liegeois-Chauvel et al. (1991, 1994). These studies did not examine in detail click-evoked responses beyond about 300 ms after stimulus onset, where we recorded several large deflections with peak latency around 400–500 ms and 1000–1100 ms.

Superimposed on these relatively large, low-frequency field potentials were far smaller AEP deflections time-locked to the individual clicks in the 100 Hz click train (i.e. FFR). The amplitudes of both the all-pass AEP and the FFR fell systematically with distance from the site of maximal amplitude on posteromedial HG, suggesting that they may arise from the same afferent supply and possibly even the same neural circuitry in the cortex. Although we do not have similar data for auditory fields beyond those described here, the FFR to 100 Hz clicks may be confined to core auditory cortex in human and thus serve as a sensitive physiological marker of this field. Lee et al. (1984) earlier recorded a frequency-following response to 40 Hz click trains on the lateral STG surface of human, and interpreted this activity as arising from HG deep within the Sylvian fissure. In both the rhesus (Steinschneider et al., 1998) and marmoset (Lu et al., 2001) monkey stimulus-synchronized responses of AI neurons to click trains have been reported at clicks rates that could reach, or even exceed, 100 Hz. In our previous study we noted frequency-following in posteromedial HG to 100 Hz click trains and to the fundamental frequency of speech sounds (Steinschneider et al., 1999) but did not attempt to map it systematically, as we have here. Thus, it may be that AI (and/or other core fields) in monkey and human represent the temporal properties of complex sound in similar ways. Whether or not the frequency range over which stimulus-synchrony is exhibited is similar in monkey and human is yet to be determined. Work is currently underway to determine the range of click frequency over which stimulus-synchrony is exhibited in the auditory core and to test whether an FFR is evoked in the other two fields identified in this paper exhibit FFR at click frequencies below the 100 Hz used in this study. Results of these studies will provide insight into possible temporal mechanisms that might be involved in the processing of pitch information (see Steinschneider et al., 1998). We are also studying the extent to which the synchrony exhibited by the human auditory core to clicks can be generalized to other amplitude modulated sounds, including running speech.

The weight of the data strongly supports the notion that this field on posteromedial HG corresponds, at least in part, to the koniocortical field(s) identified in material stained for Nissl bodies, myelinated axons or various metabolic markers. It is also most likely that it is homologous

to a greater or lesser extent with the core field of non-human primates (reviewed by Hackett, 2003). Core auditory cortex in human, as in the non-human primate, may be composed of more than one primary-like field, based on cyto- and chemo-architecture (Galaburda and Sanides, 1980; Morosan et al., 2001; Wallace et al., 2002) and fMRI tonotopic mapping (e.g. Formisano et al., 2003; Talavage et al., 2004). While Liegeois-Chauvel et al. (1994) have interpreted some of their results obtained with click stimulation in this way, there is little in our data to suggest such a functional segregation. The cytoarchitectural studies Galaburda and Sanides (1980) and Morosan et al. (2001) suggested, respectively, two or three possible primary or primary-like areas adjacent to one another on the long axis in HG. It seems highly unlikely that the electrode trajectories in our experiments did not cross boundaries between presumed core subdivisions, yet we saw no physiological evidence for such parcellation. Instead, our core area exhibited at one recording site an AEP having relatively low threshold and high amplitude, which was flanked by AEP threshold and amplitude gradients that, anterolaterally, extended to what we interpret to be the lateral boundary of the auditory core. Nor did we see any sharp transition caudomedial to the core in those experiments where the electrode penetrated most deeply into HG where it may have encountered a field adjacent to the insula. This region could contain a medial belt region or the 'root' area described by Fullerton and Pandya (2007). Energy in our click train stimulus was concentrated well below 4 kHz, and considering the fact that our mapping was done at sensation levels some 50–60 dB above hearing threshold it is not likely on acoustic grounds that we overlooked activity in the low frequency representation(s) in any of the fields. Our recording approach limited functional mapping to a relatively narrow strip of cortex along the long axis of HG, and because of this other functional boundaries, if and where they exist, could not be detected. A more extensive and finer-grained functional mapping, using a variety of different acoustic stimuli, is required to determine boundaries with other possible belt fields and to determine where and to what extent the core is functionally subdivided.

Anterior and lateral on HG the cortex takes on a different cellular architecture (Hackett, 2003). Wallace et al. (2002) labeled it explicitly the anterolateral belt area because its histochemical profile differed from that of the adjacent core (see also Hackett et al., 2001; Sweet et al., 2005). Using fMRI, Wessinger et al. (2001) observed a core–belt relationship in human that was reminiscent of that seen by Petkov et al. (2006) in monkey. We found that with recordings more anterolateral on HG, the shape of the all-pass AEP waveform changed rather abruptly and the FFR was no longer in evidence. These changes are consistent with both anatomical and functional imaging data, and suggest that recordings crossed a boundary region between a core field and a lateral belt area. This boundary, however, is not necessarily a sharp one, as evidenced by the

intensity dependency and amplitude gradient of the AEP along the long axis of posteromedial HG. Rather it would appear that there is a transition zone between the core field on posteromedial HG and the more anterolateral belt area.

It is also noted that the amplitude gradient observed in the auditory core lies on the high-to-low-frequency tonotopic axis (Howard et al., 1996b), and thus the core–belt boundary on HG would tend to lie in the vicinity of the low-frequency representation. Steinschneider et al. (1998) have reported that in the low frequency representation of AI of the rhesus monkey the upper limit for temporal synchrony of multiunit activity to click-train stimuli is around 100 Hz, which is demonstrably below that exhibited in the high-frequency representation. Whether such a direct relationship exists between temporal synchrony and tonotopy in auditory core of human is yet to be determined.

At suprathreshold levels, AEP deflections recorded anterolateral to the core field, when in evidence, were very small within the first 50 ms of stimulus onset with measurable latency not shorter than about 20 ms. When present, later waves had peak latency that typically exceeded 400–500 ms after stimulus onset. Celesia (1976) reported essentially no evoked activity far laterally on HG, whereas Liegeois-Chauvel et al. (1991) did show AEPs recorded at anterior and lateral HG sites. However, the amplitude of the AEP at these locations had declined so abruptly that it became difficult to identify early deflections clearly.

The polyphasic AEPs recorded on the posterolateral exposed surface of the STG were consistent with a field PLST described earlier by Howard et al. (2000). In that study, waveforms recorded here were shown to differ from those recorded in posteromedial HG in their shape, in their sensitivity to interval between paired clicks and to general anesthesia. Like anterolateral HG, the FFR to 100 Hz clicks was also not in evidence there. Recently, we have also shown PLST to be an area that exhibits audiovisual speech interaction (Reale et al., 2007). Field PLST in human appears to correspond to, or overlap with, the posterior portion of cytoarchitectonic areas 22 of Brodmann (1909), to Tpt and PaAlt of Galaburda and Sanides (1980), and to chemoarchitectonic area STA of Rivier and Clarke (1997) and Wallace et al. (2002). Functional MRI results (Binder et al., 2000) and direct cortical recordings (Celesia et al., 1968; Liegeois-Chauvel et al., 1991; Howard et al., 2000) have shown the posterolateral STG to be strongly activated by a wide range of simple and complex sounds. We also noted originally, on the basis of click maps, that PLST may represent more than one field, and on grounds of its location with respect to auditory cortex on HG we suggested that this area (or a portion of it) be considered parabelt auditory association cortex. Sweet et al. (2005) have since identified cytoarchitectonically two fields on posterolateral STG, which they concluded were homologs of parabelt fields in the non-human primate.

In summary, the anatomical and physiological data on human auditory cortex, though far less extensive than that

for non-human primates, supports a model of multiple interconnected fields possibly arranged in some kind of hierarchical way. Homologies between human and non-human primate have yet to be firmly established save, perhaps, for an auditory core field. What we interpret to be an auditory belt field on anterolateral HG, based on its location with respect to the posteromedial auditory core, seems not to exhibit the properties of hierarchical processing of complex sound reported for belt neurons in the monkey. Whether PLST represents one or more parabelt areas, or should even be considered the homolog of the parabelt area(s) in monkey, will require extensive comparative physiological studies of humans and non-human primates. The question of what constitutes a cortical field and the problem of where to place field borders have been argued by anatomists for more than a century, and these issues are no less pertinent when considering fields from a functional point of view (for discussion see Rose, 1949; Rose and Woolsey, 1949).

Finally, because of the highly developed capacity of humans for speech and language, which involves temporal lobe operations, we might wish to consider the possibility that one or more auditory cortical areas, including for example PLST, have arisen *de novo* in human rather than being only the result of further elaboration of areas already found in non-human primates. In any event, knowing in human the full extent and functional organization of auditory cortex on the temporal lobe involved in speech, language and related sensory and cognitive functions will require a wide range of experimental approaches applied in creative complementary ways.

Acknowledgements

We wish to thank Carol Dizack for graphic art work, and Peter Luo and Haiming Chen for computer programming and electronic instrumentation. Charles Garell, Hans Bakken, Kirill Nourski participated in some of these experiments. This work was supported by NIH Grants DC-04290, HD-03352, MH-070497 and MO1-RR-59 (General Clinical Research Centers Program) and by the Hoover Fund and Carver Trust.

References

- Arezzo, J., Pickoff, A., Vaughan Jr., H.G., 1975. The sources and intracerebral distribution of auditory evoked potentials in the alert rhesus monkey. *Brain Res.* 90, 57–73.
- Bailey, P., Bonin, G., 1951. *The Isocortex of Man*. University of Illinois Press, Urbana.
- Bidet-Caulet, A., Fischer, C., Besle, J., Aguera, P.E., Giard, M.H., Bertrand, O., 2007. Effects of selective attention on the electrophysiological representation of concurrent sounds in the human auditory cortex. *J. Neurosci.* 27, 9252–9261.
- Binder, J.R., Frost, J.A., Hammeke, T.A., Bellgowan, P.S., Springer, J.A., Kaufman, J.N., Possing, E.T., 2000. Human temporal lobe activation by speech and nonspeech sounds. *Cereb. Cortex* 10, 512–528.
- Brodmann, K., 1909. *Vergleichende Loakalisationslehre der Grosshirnrinde*. J.A. Barth, Leipzig.
- Brugge, J.F., Volkov, I.O., Garell, P.C., Reale, R.A., Howard, M.A., 2003. Functional connections between auditory cortex on Heschl's gyrus and on the lateral superior temporal gyrus in humans. *J. Neurophysiol.* 90, 3750–3763.
- Brugge, J.F., Volkov, I.O., Reale, R.A., Garell, P.C., Kawasaki, H., Oya, H., Li, Q., Howard, M.A., 2005. The posteriolateral superior temporal auditory field in humans. Functional organization and connectivity. In: Konig, R., Heil, P., Budinger, E., Scheich, H. (Eds.), *The Auditory Cortex – Toward a Synthesis of Human and Animal Research*. Erlbaum, Mahwah, NJ, pp. 145–162.
- Celesia, G.G., 1976. Organization of auditory cortical areas in man. *Brain* 99, 403–414.
- Celesia, G.G., Puletti, F., 1969. Auditory cortical areas of man. *Neurology* 19, 211–220.
- Celesia, G., Puletti, F., 1971. Auditory input to the human cortex during states of drowsiness and surgical anesthesia. *Electroencephalogr. Clin. Neurophysiol.* 31, 603–609.
- Celesia, G.G., Broughton, R.J., Rasmussen, T., Branch, C., 1968. Auditory evoked responses from the exposed human cortex. *Electroencephalogr. Clin. Neurophysiol.* 24, 458–466.
- Chatrian, G.E., Petersen, M.C., Lazarte, J.A., 1960. Responses to clicks from the human brain: some depth electrographic observations. *Electroencephalogr. Clin. Neurophysiol.* 12, 479–489.
- Fishman, Y.I., Volkov, I.O., Noh, M.D., Garell, P.C., Bakken, H., Arezzo, J.C., Howard, M.A., Steinschneider, M., 2001. Consonance and dissonance of musical chords: neural correlates in auditory cortex of monkeys and humans. *J. Neurophysiol.* 86, 2761–2788.
- Formisano, E., Kim, D.S., Di Salle, F., van de Moortele, P.F., Ugurbil, K., Goebel, R., 2003. Mirror-symmetric tonotopic maps in human primary auditory cortex. *Neuron* 40, 859–869.
- Fullerton, B.C., Pandya, D.N., 2007. Architectonic analysis of the auditory-related areas of the superior temporal region in human brain. *J. Comp. Neurol.* 504, 470–498.
- Galaburda, A.M., Sanides, F., 1980. Cytoarchitectonic organization of the human auditory cortex. *J. Comp. Neurol.* 190, 597–610.
- Godey, B., Schwartz, D., de Graaf, J.B., Chauvel, P., Liegeois-Chauvel, C., 2001. Neuromagnetic source localization of auditory evoked fields and intracerebral evoked potentials: a comparison of data in the same patients. *Clin. Neurophysiol.* 112, 1850–1859.
- Griffiths, T.D., Warren, J.D., Scott, S.K., Nelken, I., King, A.J., 2004. Cortical processing of complex sound: a way forward? *Trends Neurosci.* 27, 181–185.
- Hackett, T.A., 2003. The comparative anatomy of the primate auditory cortex. In: Ghazanfar, A.A. (Ed.), *Primate Audition: Ethology and Neurobiology*. CRC Press, Boca Raton, pp. 199–219.
- Hackett, T.A., Preuss, T.M., Kaas, J.H., 2001. Architectonic identification of the core region in auditory cortex of macaques, chimpanzees, and humans. *J. Comp. Neurol.* 441, 197–222.
- Hickok, G., Poeppel, D., 2004. Dorsal and ventral streams: a framework for understanding aspects of the functional anatomy of language. *Cognition* 92, 67–99.
- Hickok, G., Poeppel, D., 2007. The cortical organization of speech processing. *Nat. Rev. Neurosci.* 8, 393–402.
- Howard, M.A., Volkov, I.O., Granner, M.A., Damasio, H.M., Ollendieck, M.C., Bakken, H.E., 1996a. A hybrid clinical-research depth electrode for acute and chronic in vivo microelectrode recording of human brain neurons. Technical note. *J. Neurosurg.* 84, 129–132.
- Howard, M.A., Volkov, I.O., Abbas, P.J., Damasio, H., Ollendieck, M.C., Granner, M.A., 1996b. A chronic microelectrode investigation of the tonotopic organization of human auditory cortex. *Brain Res.* 724, 260–264.
- Howard, M.A., Volkov, I.O., Mirsky, R., Garell, P.C., Noh, M.D., Granner, M., Damasio, H., Steinschneider, M., Reale, R.A., Hind, J.E., Brugge, J.F., 2000. Auditory cortex on the posterior superior temporal gyrus of human cerebral cortex. *J. Comp. Neurol.* 416, 76–92.
- Kaas, J.H., Hackett, T.A., 2000. Subdivisions of auditory cortex and processing streams in primates. *Proc. Natl. Acad. Sci. USA* 97, 11793–11799.

- Lee, Y.S., Lueders, H., Dinner, D.S., Lesser, R.P., Hahn, J., Klem, G., 1984. Recording of auditory evoked potentials in man using chronic subdural electrodes. *Brain* 107, 115–131.
- Leonard, C.M., Puranik, C., Kuldau, J.M., Lombardino, L.J., 1998. Normal variation in the frequency and location of human auditory cortex landmarks. Heschl's gyrus: where is it? *Cereb. Cortex* 8, 397–406.
- Liegeois-Chauvel, C., Musolino, A., Chauvel, P., 1991. Localization of the primary auditory area in man. *Brain* 114, 139–151.
- Liegeois-Chauvel, C., Musolino, A., Badier, J.M., Marquis, P., Chauvel, P., 1994. Evoked potentials recorded from the auditory cortex in man: evaluation and topography of the middle latency components. *Electroencephalogr. Clin. Neurophysiol.* 92, 204–214.
- Lu, T., Liang, L., Wang, X., 2001. Temporal and rate representations of time-varying signals in the auditory cortex of awake primates. *Nat. Neurosci.* 4, 1131–1138.
- Morosan, P., Rademacher, J., Schleicher, A., Amunts, K., Schormann, T., Zilles, K., 2001. Human primary auditory cortex: cytoarchitectonic subdivisions and mapping into a spatial reference system. *Neuroimage* 13, 684–701.
- Petkov, C.I., Kayser, C., Augath, M., Logothetis, N.K., 2006. Functional imaging reveals numerous fields in the monkey auditory cortex. *PLoS Biol.* 4, e215.
- Puletti, F., Cellesia, G.G., 1970. Functional properties of the primary cortical auditory area in man. *J. Neurosurg.* 32, 244–247.
- Rademacher, J., Caviness, V., Steinmetz, H., Galaburda, A., 1993. Topographical variation of the human primary cortices; implications for neuroimaging, brain mapping and neurobiology. *Cereb. Cortex* 3, 313–329.
- Rademacher, J., Morosan, P., Schormann, T., Schleicher, A., Werner, C., Freund, H.J., Zilles, K., 2001. Probabilistic mapping and volume measurement of human primary auditory cortex. *Neuroimage* 13, 669–683.
- Rauschecker, J.P., 1998. Cortical processing of complex sounds. *Curr. Opin. Neurol.* 8, 516–521.
- Rauschecker, J.P., Tian, B., 2000. Mechanisms and streams from processing what and where in auditory cortex. *Proc. Nat. Acad. Sci.* 97, 11800–11806.
- Reale, R.A., Calvert, G.A., Thesen, T., Jenison, R.L., Kawasaki, H., Oya, H., Howard, M.A., Brugge, J.F., 2007. Auditory-visual processing represented in the human superior temporal gyrus. *Neuroscience* 145, 162–184.
- Rivier, F., Clarke, S., 1997. Cytochrome oxidase, acetylcholinesterase, and NADPH-diaphorase staining in human supratemporal and insular cortex: evidence for multiple auditory areas. *Neuroimage* 6, 288–304.
- Rose, J.E., 1949. The cellular structure of the auditory region of the cat. *J. Comp. Neurol.* 91, 409–440.
- Rose, J.E., Woolsey, C.N., 1949. The relations of thalamic connections, cellular structure and evocable electrical activity in the auditory region of the cat. *J. Comp. Neurol.* 91, 441–466.
- Scott, S.K., 2005. Auditory processing – speech, space and auditory objects. *Curr. Opin. Neurobiol.* 15, 197–201.
- Sem-Jacobsen, C.W., Petersen, M.C., Dodge Jr., H.W., Lazarte, J.A., Holman, C.B., 1956. Electroencephalographic rhythms from the depths of the parietal, occipital and temporal lobes in man. *EEG Clin. Neurophysiol.* 8, 263–278.
- Steinschneider, M., Reser, D.H., Fishman, Y.I., Schroeder, C.E., Arezzo, J.C., 1998. Click train encoding in primary auditory cortex of the awake monkey: evidence for two mechanisms subserving pitch perception. *J. Acoust. Soc. Am.* 104, 2935–2955.
- Steinschneider, M., Volkov, I.O., Noh, M.D., Garell, P.C., Howard III, M.A., 1999. Temporal encoding of the voice onset time phonetic parameter by field potentials recorded directly from human auditory cortex. *J. Neurophysiol.* 82, 2346–2357.
- Steinschneider, M., Volkov, I.O., Fishman, Y.I., Oya, H., Arezzo, J.C., Howard III, M.A., 2005. Intracortical responses in human and monkey primary auditory cortex support a temporal processing mechanism for encoding of the voice onset time phonetic parameter. *Cereb. Cortex* 15, 170–186.
- Steinschneider, M., Tenke, C.E., Schroeder, C.E., Javitt, D.C., Simpson, G.V., Arezzo, J.C., Vaughn, H.G., 1992. Cellular generators of the cortical auditory evoked potential initial component. *Electroencephalogr. Clin. Neurophysiol.* 84, 196–200.
- Sweet, R.A., Dorph-Petersen, K.A., Lewis, D.A., 2005. Mapping auditory core, lateral belt, and parabelt cortices in the human superior temporal gyrus. *J. Comp. Neurol.* 491, 270–289.
- Talavage, T.M., Sereno, M.I., Melcher, J.R., Ledden, P.J., Rosen, B.R., Dale, A.M., 2004. Tonotopic organization in human auditory cortex revealed by progressions of frequency sensitivity. *J. Neurophysiol.* 91, 1282–1296.
- Trebuchon-Da Fonseca, A., Giraud, K., Badier, J.M., Chauvel, P., Liegeois-Chauvel, C., 2005. Hemispheric lateralization of voice onset time (VOT) comparison between depth and scalp EEG recordings. *Neuroimage* 27, 1–14.
- Wallace, M.N., Johnston, P.W., Palmer, A.R., 2002. Histochemical identification of cortical areas in the auditory region of the human brain. *Exp. Brain Res.* 143, 499–508.
- Wessinger, C.M., VanMeter, J., Tian, B., Van Lare, J., Pekar, J., Rauschecker, J.P., 2001. Hierarchical organization of the human auditory cortex revealed by functional magnetic resonance imaging. *J. Cogn. Neurosci.* 13, 1–7.
- Yvert, B., Fischer, C., Bertrand, O., Pernier, J., 2005. Localization of human supratemporal auditory areas from intracerebral auditory evoked potentials using distributed source models. *Neuroimage* 28, 140–153.
- Yvert, B., Fischer, C., Guenot, M., Krolak-Salmon, P., Isnard, J., Pernier, J., 2002. Simultaneous intracerebral EEG recordings of early auditory thalamic and cortical activity in human. *Eur. J. Neurosci.* 16, 1146–1150.